PNAS
www.pnas.org

Supplementary Information for

IL-4/STAT6 signaling facilitates innate hematoma resolution and neurological recovery after hemorrhagic stroke in mice

Jing Xu, Zhouqing Chen, Fang Yu, Huan Liu, Cheng Ma, Di Xie, Xiaoming Hu, Rehana K. Leak, Sherry HY Chou, R. Anne Stetler, Yejie Shi, Jun Chen, Michael V. L. Bennett, and Gang Chen

Corresponding authors: Michael V. L. Bennett and Gang Chen

Email: michael.bennett@einstein.yu.edu (M.V.L.B.), nju_neurosurgery@163.com (G.C.).

This PDF file includes:

www.pnas.org/cgi/doi/10.1073/pnas.2018497117

Supplementary Methods

Animals

C57BL/6J WT and STAT6 knockout (Cat #005977, C57BL/6J background) male and female mice were purchased from the Jackson Laboratory. ST2 KO mice (1), a gift from A. McKenzie (Medical Research Council as part of UKRI, U.K), were bred for experimental use at the University of Pittsburgh. To minimize the potential influence of genetic heterogeneity on the stroke model, ST2 KO mice (originally on the 129 background) were backcrossed to the C57BL/6 background for eight generations before use. All mice were housed in a temperature and humidity-controlled animal facility with a 12-h light/12-h dark cycle. Food and water were available *ad libitum*. All animal procedures were approved by the University of Pittsburgh Institutional Animal Care and Use Committee and performed in accordance with the *Guide for the Care and Use of Laboratory Animals* (2). All efforts were made to minimize animal suffering and the number of animals used.

Models of intracerebral hemorrhage

ICH was induced in adult male or female mice (8-12 weeks old, 25-30 g) or aged male (18 months old) mice. Mice were anesthetized with 3% (vol/vol) isoflurane in 67%:33% (vol/vol) N_2O/O_2 until unresponsive to the tail pinch test. Mice were then fitted with a nose cone blowing 1.5% (vol/vol) isoflurane for anesthesia maintenance on a stereotaxic frame. ICH was induced by stereotaxic injection of either donor blood or collagenase into the right striatum. A 1 mm diameter hole was drilled in the skull (0.2 mm anterior and 2 mm lateral to Bregma), and a 28-gauge stainless steel cannula was inserted for blood/collagenase infusion into the right striatum (3.5 mm below the skull). For the collagenase injection model (3), 1 μl of 0.05U type VII-S collagenase (C2399, Sigma-Aldrich) in TESCA buffer (50 mM N-tris-(hydroxymetryl-2-amino-ethanesulfonic acid, 0.36 mM $CaCl_2$ in ddH2O, pH = 7.4) was injected. For the blood injection model (4), 30 μl whole blood was collected from mouse donors (with the same sex and same genetic background as the recipient) under isoflurane anesthesia with extracorporeal cardiac puncture without anti-coagulants. The blood was injected into the recipient mice immediately after withdrawal from the donor. Blood was injected at a rate of 2 μl/min. When the injection was completed, the cannula was left in place for 10 min. The needle was slowly withdrawn in 2 steps with a 5-min interval. Rectal temperature was maintained at 37.0 ± 0.5°C during surgery through a temperature-controlled heating pad. Mean arterial blood pressure was monitored during surgery by a tail cuff. Sham-operated animals underwent the same anesthesia and surgical procedures without intrastriatal injection.

Intranasal administration of IL-4

To make IL-4 nanoparticles, lecithin (150 mg) and cholesterol (15 mg) were dissolved in 5 mL of a chloroform-methanol mixed solution (3:1, vol/vol). A lipid layer was formed after evaporating the mixed solvent under vacuum distillation. Recombinant IL-4 protein (1 mg, Peprotech, Rocky

Hill, NJ; endotoxin level less than 0.01 ng/μg of protein) was dissolved in 5 mL of water, and then added to the lipid layer for hydration for 30 min. The mixture was homogenized by ultrasonic probes for 15 min in an ice bath and then filtered through a 0.45 μm membrane. The free IL-4 protein was removed by ultrafiltration with centrifugal filter units (100 KDa cutoff). IL-4 nanoparticles were then resuspended. The particle size and zeta potential of IL-4 protein-loaded liposomes were determined by dynamic light scattering (DLS) and electrophoretic light scattering, respectively, using Zetasizer Nano ZS instrument. The concentration of IL-4 protein in the nanoparticles was determined by the bicinchoninic protein determination kit (Thermo Fisher Scientific, Pittsburgh, PA).

After ICH or sham operation, mice were randomly and blindly assigned to receive IL-4 or vehicle nanoparticle treatment. Mice were anesthetized as described above and placed in a horizontal position with ventral side facing up. IL-4 (50 μg/kg body weight) or vehicle nanoparticles were administered intranasally. The solution was applied into each nostril 3 times (~5 μL into each nostril for each infusion) with an application interval of 5 minutes. Animals in the vehicle control group received an equal volume of vehicle nanoparticles using the same regimen. The first IL-4 administration was delivered 2 hours after ICH induction, followed by identical dosing regimen every day for the following 7 days.

MRI scanning and analyses

Both T2- and T2*-weighted images were acquired and quantified by a blinded observer (5). Mice were anesthetized via a nose cone with 1-2% isoflurane delivered in Air/O_2 (2:1). The mice were then positioned on an animal bed and placed in the scanner. A rectal temperature probe was used to monitor body temperature, which was maintained at 37.0 ± 0.5˚C using a warm air heating system. Respiration was also monitored (SA Instruments, New York, NY, USA). MRI was performed on a 9.4T/30-cm AVIII HD spectrometer (Bruker Biospin, Billerica, MA) equipped with a 12 cm high-performance gradient set, using an 86 mm quadrature RF transmit volume coil, a 2-channel receive surface RF coil, and Paravision 6.0.1. A T2-weighted RARE sequence was used to visualize the ICH brain lesion, with the following parameters: repetition time (TR)/echo time (TE) = 4000/40 ms, field of view (FOV) = 20 × 20 mm, acquisition matrix = 256 × 256, 21 slices with a slice thickness of 0.5 mm, 4 averages, and a RARE factor = 8, with an in-plane resolution of 78 μm. T2*-weighted images were collected using a FLASH sequence with the following parameters: TR/TE = 500/8 ms, FOV = 20 × 20 mm, acquisition matrix = 256 × 256, 21 slices with a slice thickness of 0.5 mm, 4 averages, and a flip angle of 25° . Data were analyzed with DSI Studio software (http://dsi-studio.labsolver.org/). Brain edema was measured from MRI coronal slices, and data calculated based on the following equation: (ipsilateral hemisphere volume – contralateral hemisphere volume)/ contralateral hemisphere volume x100%.

Measurement of the hemorrhage volume

Brains were removed and sliced into 7 equally spaced coronal sections; each 1 mm thick. The red/pink-hued hemorrhage area in lesion side was calculated using Image J by an investigator who was blinded to the experimental group assignment. The total hemorrhage volume was calculated by summing the hemorrhagic area of each section and multiplying by the thickness of each section.

Quantification of intracerebral hemorrhages

Cerebral hemorrhages were assessed by the spectrophotometric hemoglobin assay with Drabkin's reagent, as previously described (6). Briefly, mice were transcardially perfused with 50 mL ice-cold 0.9% (wt/vol) NaCl, and the brain was cut into 1-mm thick coronal sections. The brain slices were photographed, followed by sagittal separation of the left and right hemispheres along the midline. Six ipsilateral brain sections were homogenized in 500 μL water, followed by sonication on ice for 1 minute to lyse erythrocytes and other cells. Samples were centrifuged at 15,000 *g* for 30 minutes at 4°C. Supernatants were transferred to a new tube containing Drabkin's reagent, mixed well by pipetting, and incubated at 20°C for 20 minutes. Optical density values were measured by spectrophotometry at 540 nm and then calculated for hemorrhage volumes based on the standard curve by linear regression analyses. The standard curve was generated by adding 0, 0.5, 1, 2, 4, and 8 μL blood to 500 μL lysates prepared from sham brains and the optical density was measured.

Neurobehavioral tests

Foot fault test. The foot fault test was performed as described previously (7) to assess sensorimotor coordination during spontaneous locomotion. Mice were placed on an elevated metal wire (2.5 mm diameter) grid surface (30 cm [L] × 35 cm [W] × 31 cm [H]) with a grid opening of 2.25 cm^2 (1.5 cm × 1.5 cm square) and videotaped for 1 minute from beneath the grid. The videotapes were analyzed by a blinded investigator for the number of total steps and the number of foot faults made by the left limbs (impaired side, contralateral to lesion). Foot faults were determined when the mouse misplaced its impaired forepaw or hindpaw such that the paw fell through the grid. The data were expressed as percentages of foot faults over total steps by that paw. The test began 1 day before surgery, and was repeated at 3, 5, 7, and 14 days after surgery.

Adhesive removal test. The adhesive removal test was performed to assess tactile responses and sensorimotor asymmetries. Pieces of adhesive tape 2 mm x 3 mm were applied on the left paw (impaired side, contralateral to brain lesion). Tactile responses were measured by recording the time to initially contact the impaired forepaw with mouth, as well as the time to remove the adhesive tape from impaired forepaw using mouth, with a maximum observation period of 120 seconds. The test began 1 day before surgery, and was repeated at 3, 5, 7, and 14 days after surgery.

Cylinder test. The cylinder test was performed to assess forepaw use asymmetry, as described previously (8). The mouse was placed in a transparent cylinder (diameter: 9 cm; height: 15 cm)

and videotaped from the top for 8 minutes. Videotapes were analyzed in slow motion, and forepaw (left/right/both) use during the first contact against the cylinder wall after rearing and during lateral exploration was recorded. Uninjured mice typically show no preference for either forepaw, whereas injured mice display decreased use of left forepaw (impaired side; contralateral to lesion), depending on the severity of the injury. Forepaw use asymmetry was calculated with the following equation: contralateral paw use = (right-left) / (left + right + both) × 100%. The test began 1 day before surgery, and was repeated at 3, 5, 7, and 14 days after surgery.

Rotarod test. The rotarod test was performed to assess post-ICH motor functions, as described previously (9). Mice were placed on an accelerated rotating rod with the speed increasing linearly from 4 to 40 rpm within 5 minutes. On a given day each mouse was tested 3 times with an intermission of 5 minutes between tests. Latency to fall off the rotating rod was recorded. Data were expressed as mean values from the 3 trials. The tests began 1 day before surgery, and were repeated at 3, 5, 7, and 14 days after surgery.

Morris water maze. The Morris water maze test was carried out at 16-21 days after ICH, in order to evaluate spatial cognitive functions. A square platform (11 cm × 11 cm) was submerged in a pool (diameter: 109 cm) filled with water rendered opaque with nontoxic paint. In the learning phase of the test, the mouse was placed into the pool from one of the four locations and allowed to swim for up to 60 seconds to escape to the hidden platform. The time needed until the animal found the platform (escape latency) was recorded for each trial to evaluate 'spatial learning'. At the end of each trial, the mouse was allowed to remain on the platform or placed on the platform (if the mouse could not find the platform within 60 seconds) for 10 seconds with prominent spatial cues displayed around the room. Mice were pre-trained for 3 consecutive days before ICH (3 trials on each day). The results of last training data were recorded as baseline level on day -1. After ICH, 4 trials were performed on each testing day for 5 consecutive days (16-20 days after ICH). In the memory phase of the test at 21 days after ICH, a single, 60-second probe trial was performed with the platform removed. The time the mouse spent swimming in the goal quadrant where the platform was previously located was recorded as 'spatial memory' and expressed as a percentage of the total testing time (60 seconds).

Immunohistochemistry and image analysis

Mice were euthanized and transcardially perfused with 50 mL 0.9% (wt/vol) NaCl followed by 50 mL 4% (wt/vol) paraformaldehyde in PBS. Brains were harvested and cryoprotected in 30% (wt/vol) sucrose in PBS, and frozen serial coronal brain sections (25 μm thick) were prepared on a sliding microtome (Microm HM 450, Thermo Scientific, Walldorf, Germany). Sections were blocked with 5% (vol/vol) donkey serum in PBS for 1 hour, followed by overnight incubation (4°C) with the primary antibodies (**SI Appendix, Table S1**). After three washes, sections were incubated for 1 hour at 20°C with donkey secondary antibodies conjugated with DyLight 488 or Cy3 fluorophores (1:1000, Jackson ImmunoResearch Laboratories, Inc., West Grove, PA, USA). Alternate sections from each experimental condition were incubated in all solutions except the

primary antibodies to assess nonspecific secondary antibody staining. Sections were then mounted and coverslipped with Fluoromount-G containing DAPI (Southern Biotech, Birmingham, AL, USA). Fluorescence images were captured with an inverted Nikon Diaphot-300 fluorescence microscope equipped with a SPOT RT slider camera and Meta Series Software 5.0 (Molecular Devices, Sunnyvale, CA, USA), or with an Olympus Fluoview FV1000 confocal microscope and FV10-ASW 2.0 software (Olympus America, Center Valley, PA, USA).

For confocal imaging, image analyses were performed on two randomly selected microscopic fields (0.15mmx0.15mm) in the perilesional areas. Two sections covering the lesion area were assessed for each mouse brain. The recorded images were loaded onto Image J (NIH) and were manually quantified by two observers blinded to experimental grouping. Positively stained cells were electronically labelled with the software to avoid duplication of counting.

For iron staining, brain sections were washed three times with 0.3% PBST solution for 5 minutes each time. The brain sections were incubated in an iron staining working solution (1:1, 5% potassium ferrocyanide and 5% HCl) for 45 minutes and washed three times in distilled water for 5 minutes each time. Brain slices were then incubated in 0.5% diamine benzidine tetrahydrochloride for 1 hour.

Flow Cytometry

Flow cytometric analysis was performed using a FACS flow cytometer (BD Biosciences, San Jose, CA). Briefly, animals were euthanized and perfused with 50 mL cold saline. Brains were dissected and right hemispheres (the ICH side) were collected. Brain homogenates were passed through a cell strainer (70 μm, Fisher Scientific, Pittsburgh, PA). Single cell suspensions were separated from myelin and debris by Percoll (17-0891-01; GE Healthcare, Chicago) discontinuous 30%/70% gradient centrifugation (500 *g*, 30 minutes, 18°C). The mononuclear cells in the interface were collected and washed with HBSS (Sigma-Aldrich, St. Louis, MO) containing 1% FBS (Sigma-Aldrich, St. Louis, MO) and 2 mM EDTA (Sigma-Aldrich, St. Louis, MO) before staining. Cells were first stained with antibodies to surface antigens at 4°C for 30 minutes. After two washes with HBSS containing 1% FBS and 2 mM EDTA, cells were fixed and permeabilized with an intracellular staining kit (Thermo Fisher eBioscience, Pittsburgh, PA) according to the manufacturer's protocol. Cells were then stained with antibodies to intracellular proteins at room temperature for 30 minutes. After two washes, secondary antibodies were applied. For every 1 x 10^6 cells, an antibody cocktail diluted in 100 μL of HBSS with 1% FBS and 2 mM EDTA (surface marker) or 100 μL of 1x Permeabilization buffer (Thermo Fisher eBioscience, Pittsburgh, PA) (intra-cellular marker) were applied. The IgG antibodies that match primary antibody's host species and immunoglobobulin class were used as isotype control.

Primary macrophage-enriched culture

Primary macrophage-enriched cultures were prepared from the bone marrow of 8-week-old WT or STAT6 KO mice. Monocytes were isolated using a mouse monocyte isolation kit (STEMCELL Technologies, Vancouver, BC, Canada) according to manufacturer's instructions and cultured in the presence of macrophage colony-stimulating factor (M-CSF, 20 ng/ml) to induce their differentiation into macrophages. Macrophages were collected at 7 days *in vitro* for further experimentation.

Primary microglia-enriched cultures and treatments

Primary microglia-enriched cultures were prepared from whole brains of 1-day-old mixed sex Sprague-Dawley rat pups or WT and STAT6 KO mice pups, as described previously (10).

RBC isolation and labeling for phagocytosis assay

Red blood cells (RBCs) were purified using density gradient centrifugation and washed with PBS. For *in vivo* phagocytosis, $1x10^9$ purified RBC were diluted in 50 mL PBS (0.1%BSA) and incubated with 5 μM fluorescent dye 5(6)-carboxyfluorescein diacetate (CFDA; C1157, Invitrogen™, USA) in the dark at room temperature for 30 minutes. Cells were washed three times with PBS, diluted in 1 mL PBS, and used for phagocytosis *in vivo* (3, 4). For *in vitro* phagocytosis, the pHrodo™ Red E. coli BioParticles® Conjugate (P35361, Invitrogen™, USA) was prepared at 1 mg/mL in PBS at pH 7.4. One hundred microliters of purified RBC solution were diluted and incubated with pHrodo™ Red E. coli BioParticles® in the dark at room temperature for 10 minutes for phagocytosis *in vitro* (11).

In vivo and in vitro RBC phagocytosis assay

For assessments of *in vivo* phagocytosis, 30 μl CFDA-labeled RBCs were stereotaxically injected into the right striatum. Mice were sacrificed 5 days after injection and perfused with 40 mL cold PBS. Single cell suspensions were prepared using the Tissue Dissociation Kit T (130-092-628, Miltenyi Biotec, Auburn, CA) following manufacturer's instructions. Cells were placed on a 30%/70% Percoll gradient to isolate leukocytes and remove myelin. Cells were washed and stained with antibodies for cell surface markers (CD45-Percp cy5.5, CD11b-PB, Ly6G-BUV395) at room temperature for 20 minutes. RBC-engulfed cells were identified as $CFDA^+CD45^{int}CD11b^+$ cells and $CFDA^+CD45^{hi}CD11b^+$ cells.

For *in vitro* phagocytosis, primary microglia or macrophages were incubated with fluorescent-labeled RBCs (RBCs:phagocytes = 10:1) up to 4 hours. Unphagocytosed free-floating RBCs were removed by aspiration. Cells were washed with PBS and subjected to FACS or fixed with paraformaldehyde for immunofluorescence staining. Phagocytic index was calculated as percentages of RBC-containing microglia/macrophages among total numbers of microglia/macrophages.

Irradiation and bone marrow transplantation

To construct bone marrow chimeric mice, 5 week-old recipient male C57BL/6J WT and STAT6 KO mice were anesthetized and exposed to lethal gamma irradiation (950 rad, 10 minutes, single dose) with their heads shielded (12). Bone marrow cells were obtained from 8- to 10- weeks old male C57BL/6J WT, STAT6 KO, or CX3CR1-GFP donors and then intravenously transferred to recipient mice at 6 hours after irradiation (10^7 cells per recipient). Chimeric mice were allowed to recover for 6 weeks before ICH induction.

Quantitative polymerase chain reaction (PCR) array

To perform the quantitative PCR array for the detection of phagocytosis-related genes, the RT² Profiler™ Mouse PCR Array Phagocytosis assays (PAMM-173Z, QIAGEN, Valencia, CA) were performed following manufacturer's instructions. Microglia and macrophages were purified from ICH brains and sham control brains, respectively, by cell sorting using a FACS flow cytometer. Total RNA was isolated from the sorted microglia and macrophages using the RNeasy Lipid Tissue Mini kit (74804; QIAGEN, Valencia, CA) according to the manufacturer's instructions. Program for real time PCR was 95°C 15 minutes, (94°C 20s, 59°C 30s, 72°C 30s, plate read) x 40, melting curve from 50°C to 92°C, reading every 0.2°C, hold 2 s, and incubation at 8°C until program was ended. The cycle time values were normalized to GAPDH and GUSb in the same sample as internal controls. The expression levels of the mRNAs were then reported as fold change *vs.* sham brain or vehicle treated microglia/macrophages.

Statistical analyses

Datasets adhering to a Gaussian distribution are presented as mean ± SD. Individual data points are plotted where applicable. Non-normally distributed data are presented as box-and-whisker plots showing the 25^{th}, 50^{th}, and 75^{th} percentiles and the maximum and minimum values. Statistical comparison of the means between two groups of normal distribution was accomplished by the Student's *t* test (two-tailed). Mann-Whitney U rank sum test was used for continuous variables with non-normal distribution. Differences in means among multiple groups were analyzed using one or two-way ANOVA followed by the Bonferroni *post hoc* correction. The correlation analyses between continuous data with normal distribution were performed using Pearson correlation analyses. Spearman rank correlation analyses were used to test correlations between data sets with non-normal distributions. A *p* value less than 0.05 was deemed statistically significant. * or # at the right of time course measurements shows differences between two indicated lines. * or # above single days shows p values for the indicated day. All statistics were performed using GraphPad Prism 8 and summarized in **SI Appendix, Table S2**.

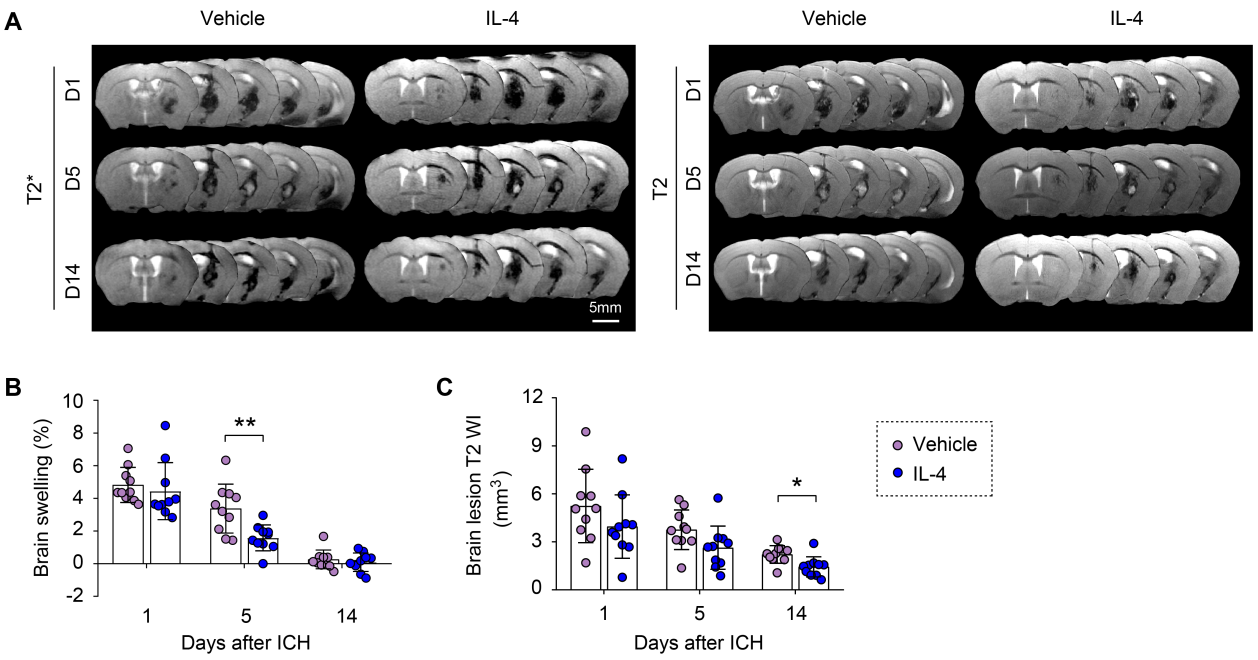

Supplemental Figure 1. Intranasal IL-4 treatment improves hematoma resolution following ICH in young male mice. ICH was induced in 10-week-old male C57/BL6 mice by unilateral, blood injection into the striatum, followed by intranasal IL-4 or vehicle nanoparticle treatment starting 2h after ICH and repeated daily for the next 7 days. **(A)** Representative axial T2* and T2 images obtained from the same mice in each group on days 1, 5, and 14 following ICH. **(B-C)** Quantification of brain lesion volumes (B) and brain swelling (C) on T2-weighted images. Data are mean±SD, n = 10/group. *p < 0.05, **p < 0.01, by two-way ANOVA repeated measurement and Bonferroni *post hoc* tests.

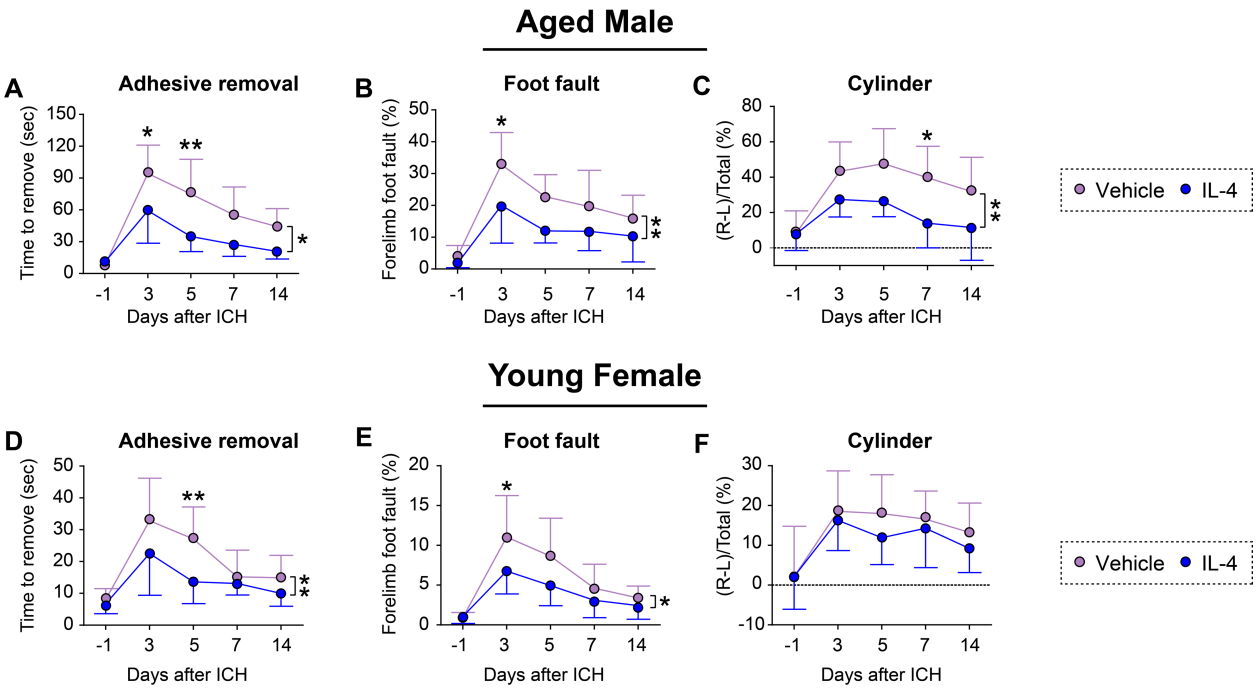

Supplemental Figure 2. Intranasal IL-4 treatment improves sensorimotor functional recovery after ICH in aged male mice and young female mice. (A-C) ICH was induced in 18-month old male C57/BL6 mice by blood injection into the right striatum, followed by intranasal IL-4 or vehicle nanoparticle treatment starting 2 hours after ICH and then repeated daily for 7 days. Sensorimotor functions were measured by adhesive removal (A), foot fault (B), and cylinder (C) tests before surgery and 3-14 days after ICH. Data are mean±SD, n =6-8/group. **(D-F)** ICH was induced in 10-week old female C57/BL6 mice by autologous blood injection into the right striatum, followed by IL-4 or vehicle treatment starting 2 hours after ICH and then repeated daily for 7 days. Sensorimotor functions were measured by adhesive removal (D), foot fault (E), and cylinder (F) tests before surgery and 3-14 days after ICH. Data are mean±SD, n = 8-9/group. *p < 0.05, **p < 0.01, by two-way ANOVA repeated measurement and Bonferroni *post hoc* tests.

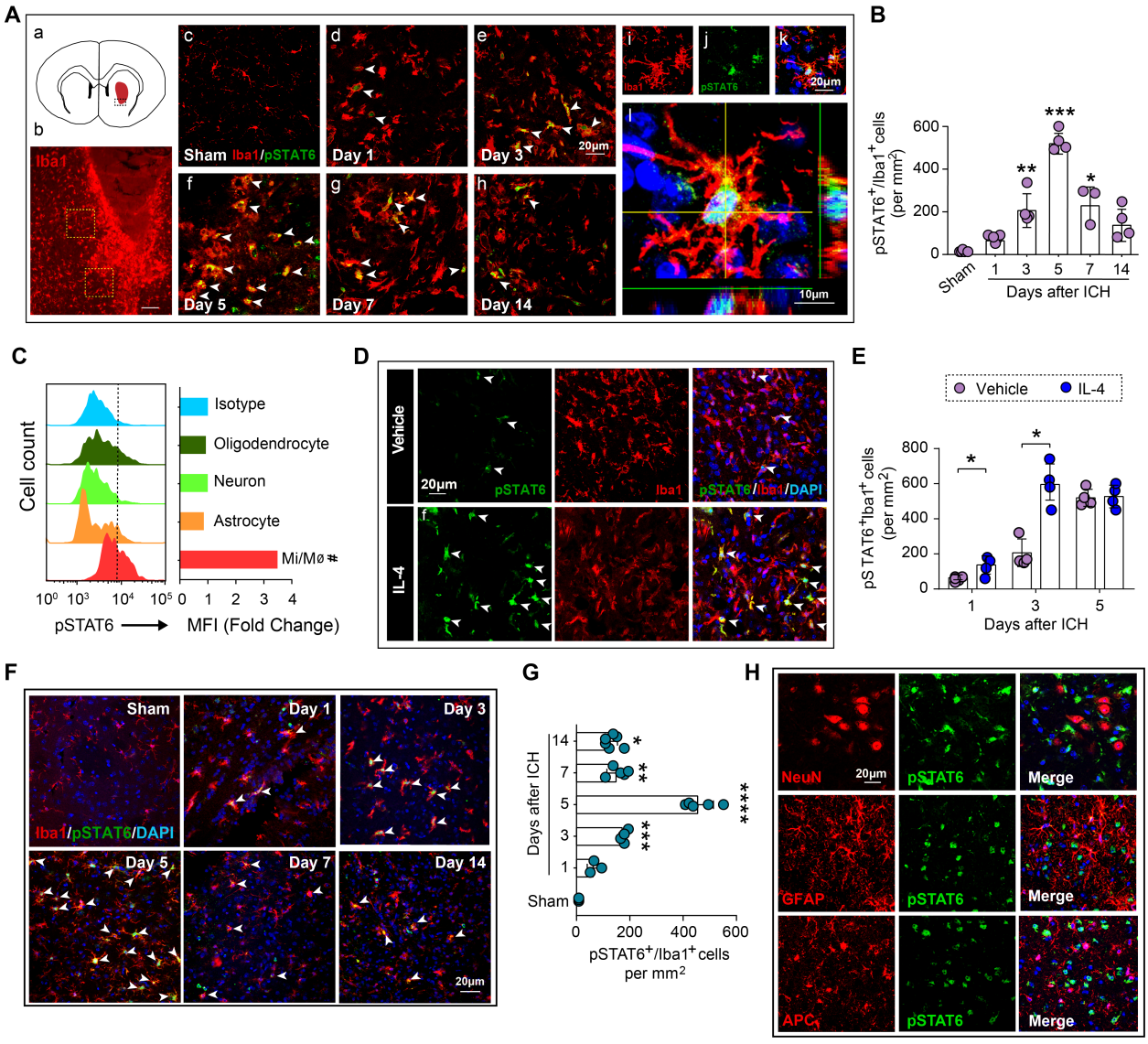

Supplemental Figure 3. STAT6 is activated in microglia/macrophages after ICH and following IL-4 treatment. (A-D) ICH was induced in WT and STAT6 KO mice by blood injection into the striatum. **(A)** Representative images of coronal brain sections showing the phosphorylation (activation) of STAT6 in microglia and macrophages at indicated time points after ICH induced by blood injection. Activated STAT6 (green) was stained with an antibody recognizing the phosphorylated (Tyrosine 641) pSTAT6. Microglia/macrophages were labeled with Iba1 (red). a. Schematic illustration shows the location of hematoma in striatum. b. The image shows low-power Iba1 (red) staining in the area in black box in (a). Yellow boxes depict the approximate locations in the peri-hematoma regions where the imaging analyses were performed. c-h. Double-label immunofluorescent images of $pSTAT6^+$ (green) in $Iba1^+$ (red) microglia/macrophages in brains collected 1-14 days after ICH and from a sham-control brain. i-k. Representative confocal images

from the peri-hematoma region of a brain slice at 3 days after ICH, showing co-localization of pSTAT6 (green) in $Iba1^+$ (red) microglia/macrophages. l. 3D reconstruction of a triple-labeled cell from i-k, showing that pSTAT6 immunofluoresnece (green) in the $Iba1^+$ (Red) cell is associated with the nucleus ($DAPI^+$, blue). **(B)** Quantification of the number of $pSTAT6^+Iba1^+$ cells in the imaging areas indicated in (A) at different time points after ICH. n = 3-5 mice per group. *p < 0.05, **p < 0.01, ***p < 0.001 vs. day 1. **(C)** Flow cytometric analysis of pSTAT6 in brain microglia/ macrophages ($CD45^+CD11b^+$), astrocytes ($CD45^-GLAST^+$), oligodendrocytes ($CD45^-O4^+$), and neurons ($CD45^-NeuN^+$) 3 days after ICH. MFI: Mean Fluorescence Intensity. Dashed line indicates the position of gating for pSTAT6 signals based on the isotype staining (the level of non-specific binding by antibodies). Data are expressed as fold changes of the mean fluorescent intensity (MFI) vs. isotype control. Iso: rabbit IgG as an isotype control for pSTAT6. n = 3-5 mice. #p < 0.0001 vs. Isotype control (mouse IgG) stained samples. **(D)** Representative images of brain sections showing STAT6 activation (green) in microglia and macrophages (Iba1) at 3 days in IL-4 or vehicle-treated ICH mice. **(E)** Quantification of the number of $pSTAT6^+Iba1^+$ cells in the imaging areas indicated in (A) at different time points after ICH. n = 4 mice per group. *p < 0.05, **p < 0.01. **(F-H)** ICH was induced in WT and STAT6 KO mice by collagenase (0.05U) injection into the striatum. **(F)** Representative images of coronal brain sections showing pSTAT6 (green) in $Iba1^+$ microglia/macrophages (red) at 1, 3, 5, 7 and 14 days after ICH or 3 days after sham operation. Arrows indicate nuclear (DAPI, blue) localization of pSTAT6 (green) in $Iba1^+$ (red) microglia/macrophages. **(G)** Quantification of the number of $pSTAT6^+Iba1^+$ cells in the peri-hematoma areas at different time points after ICH. Data are mean±SD, n = 3-6 mice/group. *p<0.05, **p < 0.01, ***p < 0.001 vs. day 1. **(H)** pSTAT6 (green) was not detected in neurons ($NeuN^+$, red), astrocytes ($GFAP^+$, red), or oligodendrocytes (APC^+, red).

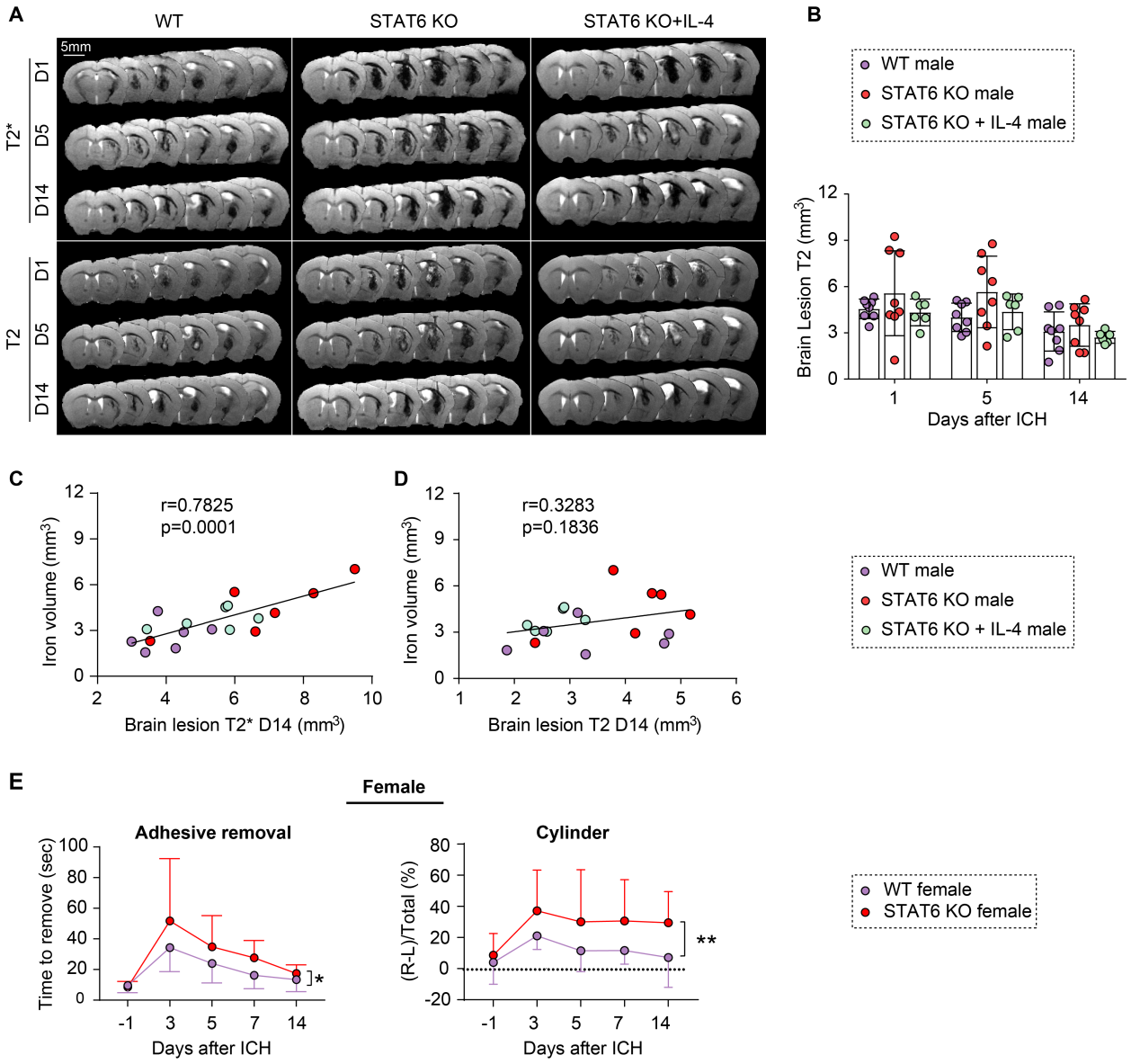

Supplemental Figure 4. STAT6 is beneficial for outcomes in the blood injection model of ICH in young male and female mice. (A-D) ICH was induced in WT and STAT6 KO young male mice (10-week-old) by blood injection into the right striatum. IL-4 or vehicle nanoparticles were intranasally applied starting 2 hours after ICH and repeated daily for 7 days. **(A)** Representative T2* and T2 images obtained from the same mice in each group at 1, 5, and 14 days after ICH. **(B)** Quantification of brain lesion volumes on T2-weighted images. Data are mean±SD, n = 6-8/group. **(C)** Pearson correlation analysis between iron$^+$ volume and brain lesion size on T2* images. **(D)** Pearson correlation analysis between iron$^+$ volume and brain lesion size on T2 images. **(E)** ICH was induced in young female WT and STAT6 KO mice (10-week-old) by blood injection into the right striatum. Sensorimotor functions were measured by adhesive removal and cylinder tests before surgery (-1 day) and 3 -14 days after ICH. n = 9-12/group. *p < 0.05, **p < 0.01 between the two groups, by two-way repeated measurement ANOVA and Bonferroni.

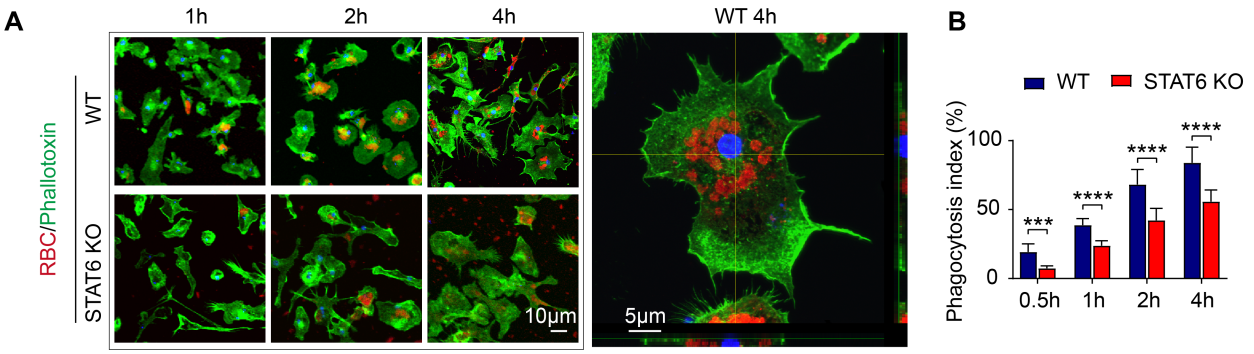

Supplemental Figure 5. STAT6 KO impairs RBC phagocytosis by microglia *in vitro*. RBCs were labeled with fluorescent dye for 10 min and then incubated with primary microglial cultures for 0.5, 1, 2, or 4 hours. **(A)** Representative images show RBC phagocytosis by WT and STAT6 KO microglia, respectively, 4 hours after RBC/microglia co-incubation. The image on the right in A (higher magnification) shows an example of robust phagocytosis by a WT cell. **(B)** Quantification as percentage of RBC-engulfing microglia at 0.5-4 hours after incubation with fluorescence-labeled RBCs. Data represent three to five independent experiments; each was performed in duplicates. ***$p < 0.001$ vs. WT by Student's *t* test, two-tailed.

Table S1. Key Reagents

REAGENT or RESOURCE	SOURCE	IDENTIFIER
Antibodies		
Rabbit Anti-STAT6 (phosphor Y641)	Abcam	ab28829
Anti-MAP2 (clone AP20)	Millipore	MAB3418
Mouse Anti-NeuN	Abcam	ab104224
Goat Anti-Iba1	Abcam	ab5076
CD11b Monoclonal Antibody, PB	eBioscience™	48-0112-82
CD45 Monoclonal Antibody, PerCP-Cyanine5.5	eBioscience™	45-0451-82
BUV395 Rat Anti-Mouse Ly-6G	BD Biosciences	563978
PE-CF594 Rat Anti-Mouse IL-4	BD Biosciences	562450
Arginase 1/ARG1 PE-conjugated Antibody	R&D Systems'	5868P
TNF alpha Monoclonal Antibody, APC	eBioscience™	17-7321-82
Alexa Fluor® 488 Rat Anti-Mouse IL-6	BD Biosciences	561363
APC-Cy™7 Rat Anti-Mouse Ly-6C	BD Biosciences	560596
PE Mouse Anti- Stat6 (pY641)	BD Biosciences	612701
Anti-O4 APC	Miltenyi Biotec	130-119-155
Anti-MAP2	Abcam	Ab32454
Anti-Glast-PE	Miltenyi Biotec	130-118-344
APC anti-mouse ST2 antibody	Biolegend	146605
Anti-GFAP antibody	Abcam	Ab53554
Protein APC Monoclonal Antibody	Invitrogen	MA1-72530
Chemicals, Peptides, and Recombinant Proteins		
Collagenase from Clostridium histolyticum	Sigma-Aldrich	C2399
Recombinant IL-4 protein	Peprotech	214-14
pHrodo™ Red E. coli BioParticles® Conjugate	Invitrogen™	P35361
CFSE	Invitrogen™	C1157
Iron Stain Kit	Sigma-Aldrich	HT20-1KT
Diaminobenzidine tetrahydrochloride	Sigma-Aldrich	D5905
Critical Commercial Assays		
Drabkin's reagent	Sigma-Aldrich	D5941
RT^2 Profiler PCR Array Mouse Phagocytosis	QIAGEN	PAMM-173Z

Table 2 Statistical Table

FIGURE 1	n	DATA STRUCTURE	TEST USED	STATISTIC	P VALUE
1B	*Vehicle=10, IL-4=10*	*Normal distribution*	*2-way repeated ANOVA, Bonferroni post hoc*	*F(1,18)=2.625*	*p(D1)>0.9999, p(D5)=0.0859, p(D14)=0.0085*
1C	*Vehicle=10, IL-4=10*	*D1-D5, D5-D14: Normal distribution; D1-D14: IL-4 non normal distribution*	*D1-D5, D5-D14: t test; D1-D14: Mann-Whitney U test*	*D1-D5: t=3.431, D5-D14: t=1.249, D1-D14: u=22*	*p(D1-D5)=0.0030, p(D5-D14)=0.2276, p(D1-D14)=0.0355*
1D	*D1: vehicle=8, IL-4=6; D5: vehicle=8, IL-4=7; D7: vehicle=8, IL-4=8*	*Normal distribution*	*t test*	*D1: t=0.878604 ; D5: t=2.81271; D7: t=2.24374*	*p(D1)=0.3969, p(D5)=0.0147; p(D7)=0.0415*
1E	*D1: vehicle=10, IL-4=8; D5: vehicle=8, IL-4=8; D7: vehicle=8, IL-4=8*	*Normal distribution*	*t test*	*D1: t=0.4468; D5: t=2.17305; D7: t=2.21597*	*p(D1)=0.6610; p(D5)=0.0474; p(D7)=0.0438*
1F	*Vehicle=10, IL-4=11*	*Normal distribution*	*t test*	*T=2.55380*	*p=0.0194*
1G	*Vehicle=10, IL-4=11*	*Normal distribution*	*2-way repeated ANOVA, Bonferroni post hoc*	*F(1,19)=9.326*	*p=0.0065; p(D1)=0.9889, p(D3)=0.6309, p(D5)=0.0591, p(D7)=0.0148, p(D14)=0.0098*
1H	*Vehicle=10, IL-4=11*	*Non-normal distribution*	*2-way repeated ANOVA, Bonferroni post hoc*	*F(1,19)=5.997*	*p=0.0242, p(D1)>0.9999, p(D3)=0.6070, p(D5)=0.2045, p(D7)=0.4831, p(D14)=0.4604*
1I	*Vehicle=10, IL-4=11*	*Non-normal distribution*	*2-way repeated ANOVA, Bonferroni post hoc*	*F(1,19)=5.592*	*p=0.0288, p(D1)>0.9999, p(D3)=0.6735, p(D5)=0.3985, p(D7)=0.1723, p(D14)=0.2457*
1J	*Vehicle=8, IL-4=8*	*Non-normal distribution*	*2-way repeated ANOVA, Bonferroni post hoc*	*F(1,14)=4.899*	*p=0.0440, p(D1)>0.9999, p(D16)>0.9999, p(D17)=0.2958, p(D18)=0.5287, p(D19)=0.3342, p(D20)=0.1069*
Time in target	*Vehicle=8, IL-4=8*	*Normal distribution*	*t test*	*t=2.79503*	*p=0.0143*
1K	*Vehicle=10, IL-4=10*	*AR d14: non-normal distribution, T2* d14: normal distribution*	*Spearman correlation*	*R=0.6185*	*p=0.0036*
1L	*Vehicle=10, IL-4=10*	*Normal distribution*	*Pearson correlation*	*R=0.4896*	*p=0.0285*
1M	*Vehicle=10, IL-4=10*	*AR d14: non-normal distribution, Clearance d1-d5%: normal distribution*	*Spearman correlation*	*R=-0.5169*	*p=0.0196*
1N	*Vehicle=10, IL-4=10*	*Non-normal distribution*	*Spearman correlation*	*R=-0.3649*	*p=0.1136*

FIGURE 2	n	DATA STRUCTURE	TEST USED	STATISTIC	P VALUE

2B	*WT=8, KO=8, KO+IL-4=6*	*Normal distribution*	*2-way repeated ANOVA, Bonferroni post hoc*	*F(2,19)=7.932*	*p=0.0031 D1: WT vs KO p>0.999; WT vs KO+IL-4 p>0.999; KO vs KO+IL-4 p>0.999; D5: WT vs KO p=0.0432; WT vs KO+IL-4 p=0.1084; KO vs KO+IL-4 p=0.3130; D14: WT vs KO p=0.0135; WT vs KO+IL-4 p=0.0720; KO vs KO+IL-4 p=0.5872;*
2C	*WT=6, KO=6, KO+IL-4=6*	*Normal distribution*	*1-way ANOVA, Tukey post hoc*	*F(2,15)=3.628*	*p=0.0519, p(KO vs WT)=0.0425, p(WT vs KO+IL-4)=0.2970, p(KO vs KO+IL-4)=0.5093*
2D	*WT=8, KO=8, KO+IL-4=8*	*Non normal distribution*	*2-way repeated ANOVA, Bonferroni post hoc*	*F(2,21)=4.690*	*p=0.0107, WT vs KO: p=0.0041, WT vs KO+IL-4: p=0.0023, KO vs KO+IL-4: p>0.9999; D1: WT vs KO p>0.9999, WT vs KO+IL-4 p>0.9999, KO vs KO+IL-4 p>0.9999; D3: WT vs KO p=0.0095, WT vs KO+IL-4 p=0.3197, KO vs KO+IL-4 p=0.4993; D5: WT vs KO p=0.0052, WT vs KO+IL-4 p=0.0462, KO vs KO+IL-4 p>0.9999; D7: WT vs KO p=0.0019, WT vs KO+IL-4 p=0.2313, KO vs KO+IL-4 p=0.2552; D14: WT vs KO p=0.5897, WT vs KO+IL-4 p=0.1326, KO vs KO+IL-4 p>0.9999*
2E	*WT=8, KO=8, KO+IL-4=8*	*Non normal distribution*	*2-way repeated ANOVA, Bonferroni post hoc*	*F(2,21)=9.707*	*p=0.0010, WT vs KO: p<0.0001, WT vs KO+IL-4: p=0.0002, KO vs KO+IL-4: p=0.9726; D1: KO vs WT p >0.9999, WT vs KO+IL-4 p>0.9999, KO vs KO+IL-4 p>0.9999; D3: KO vs WT p=0.0008, WT vs KO+IL-4 p<0.0001, KO vs KO+IL-4 p=0.8240; D5: KO vs WT p=0.0228, WT vs KO+IL-4 p=0.002, KO vs KO+IL-4 p>0.9999; D7: KO vs WT p=0.0214, WT vs KO+IL-4 p=0.1245, KO vs KO+IL-4>0.9999; D14: KO vs WT p=0.0326, WT vs KO+IL-4 p=0.0429, KO vs KO+IL-4 p>0.9999*
2F	*WT=8, KO=8, KO+IL-4=6*	*FF d14: normal distribution, T2* d14: non normal distribution*	*Spearman correlation*	*R=0.4846*	*p=0.0223*

FIGURE 3	**n**	**DATA STRUCTURE**	**TEST USED**	**STATISTIC**	**P VALUE**
3B	*D1: WT=8, KO=8; D5: WT=13, KO=12; D7: WT=10, KO=10*	*D1: WT non normal distribution, KO normal distribution; D5: normal distribution; D7: normal distribution*	*D1: Mann-Whitney test; D5: t test; D7: t test*	*U(D1)=28; t(D5)=2.599; t(D7)=3.024*	*p(D1)=0.7209, p(D5)=0.0160, p(D7)=0.0073*

3C	*D1: WT=8, KO=8;
	D5: WT=13, KO=12;
	D7: WT=10, KO=10*
		*D1: normal distribution;
		D5: normal distribution;
		D7: normal distribution*
			*D1: t test;
			D5: t test;
			D7: t test*
				*t(D1)=0.02006;
				t(D5)=2.655;
				t(D7)=2.315*
					*p(D1)=0.9843,
					p(D5)=0.0142,
					p(D7)=0.0326*

3D	*WT sham=6, STAT6 KO sham=6, WT=12, STAT6 KO=12*	*Normal distribution*	*2-way repeated ANOVA, Bonferroni post hoc*	*F(3,32)=15.63*	*p<0.0001, WT sham vs KO sham: p>0.9999, WT sham vs WT ICH: p=0.0326, KO sham vs KO ICH: p<0.0001, WT ICH vs KO ICH: p=0.0114; Pre: WT ICH vs KO ICH p>0.9999,*

					D3: WT ICH vs KO ICH p=0.0833, D5: WT ICH vs KO ICH p=0.0127, D7: WT ICH vs KO ICH p=0.0035, D9: WT ICH vs KO ICH p=0.0118, D11: WT ICH vs KO ICH p=0.0049
3F	*WT sham=6, STAT6 KO sham=6, WT=12, STAT6 KO=12*	*Non normal distribution*	*2-way repeated ANOVA, Bonferroni post hoc*	*F(3,32)=7.159*	*p=0.0008, WT sham vs KO sham: p>0.9999; WT ICH vs WT sham: p=0.5057, KO ICH vs KO sham: p=0.0038, WT ICH vs KO ICH: p=0.1212, Pre: WT ICH vs KO ICH p>0.9999, D16: WT ICH vs KO ICH p>0.9999, D17: WT ICH vs KO ICH p=0.6977, D18: WT ICH vs KO ICH p=0.0094, D19: WT ICH vs KO ICH p=0.0401, D20: WT ICH vs KO ICH p=0.1257.*
3G	*WT sham=6, STAT6 KO sham=6, WT=12, STAT6 KO=12*	*Normal distribution*	*1-way ANOVA, Bonferroni post hoc*	*F(3, 32)=5.450*	*p=0.0038, WT sham vs KO sham: p>0.9999, WT sham vs WT ICH: p>0.9999, KO sham vs KO ICH: p=0.1876, WT ICH vs KO ICH: p=0.0089*
3H	*WT sham=6, STAT6 KO sham=6, WT=12, STAT6 KO=12*	*Normal distribution*	*1-way ANOVA, Tukey post hoc*	*F(3,32)=4.212*	*p=0.0128, WT sham vs KO sham: p>0.9999, WT sham vs WT ICH: p=0.3306, KO sham vs KO ICH: p=0.0632, WT ICH vs KO ICH: p>0.9999.*

FIGURE 4	**n**	**DATA STRUCTURE**	**TEST USED**	**STATISTIC**	**P VALUE**
4C	*WT=6, KO=6*	*WT: non normal distribution, KO: normal distribution*	*Mann-Whitney test*	*U=2*	*p=0.0087*
4D	*WT=6, KO=6*	*Normal distribution*	*t test*	*t=1.371*	*p=0.2004*
4G	*Macrophage: WT=6, KO=6; Microglia: WT=5, KO=5*	*Normal distribution*	*t test*	*t(MP)=3.303, t(MG)=2.398*	*p(MP)=0.0080 p(MG)=0.043*

FIGURE 5	**n**	**DATA STRUCTURE**	**TEST USED**	**STATISTIC**	**P VALUE**
5A	*WT=7, KO=7*	*Normal distribution*	*t test*	*t=4.436*	*p=0.0008*
5B	*WT=7, KO=7*	*Normal distribution*	*t test*	*t=1.293*	*p=0.2203*
5E	*WT=8, KO=7*	*Normal distribution*	*t test*	*t(arg1)=2.176, t(il4)=2.287, t(il6)=0.9320, t(tnfa)=1.231*	*p(arg1)=0.0486, p(il4)=0.0396, p(il6)=0.3683, p(tnfa)=0.2401*
5F	*WT=9, KO=8*	*Non normal distribution*	*Mann-Whitney test*	*U(arg1)=22, U(il4)=31, U(il6)=21, U(tnfa)=25*	*p(arg1)=0.1996, p(il4)=0.6730, p(il6)=0.1592, p(tnfa)=0.3213*

FIGURE 6	**n**	**DATA STRUCTURE**	**TEST USED**	**STATISTIC**	**P VALUE**
6B	*GFP+ =10, GFP- =10*	*Normal distribution*	*t test*	*t=4.512*	*p=0.0003*
6E	*WT/WT=10, WT/KO=10,*	*Normal distribution*	*2-way repeated ANOVA, Bonferroni post hoc*	*F(2,28)=4.109*	*P=0.0273, WT/WT vs WT/KO: p=0.0415,*

	KO/WT=11				*WT/WT vs KO/WT: p=0.0234, WT/KO vs KO/WT: p>0.9999; D5: WT/WT vs WT/KO p=0.0453, WT/WT vs KO/WT p=0.0365, WT/KO vs KO/WT p>0.9999; D7: WT/WT vs WT/KO p=0.095, WT/WT vs KO/WT p=0.0584, WT/KO vs KO/WT p>0.9999*
6F	*WT/WT=10, WT/KO=10, KO/WT=11*	*Normal distribution*	*1-way ANOVA Bonferroni post hoc*	*F=13.13*	*P<0.0001, WT/WT vs WT/KO: p=0.0238, WT/WT vs KO/WT: p<0.0001 WT/KO vs KO/WT: p=0.0937*

FIGURE7	**n**	**DATA STRUCTURE**	**TEST USED**	**STATISTIC**	**P VALUE**
7B	*KO/KO=6, WT/KO=6*	*Normal distribution*	*2-way repeated ANOVA, Bonferroni post hoc*	*F(1,10)=6.374*	*p(D1)>0.9999, p(D5)=0.0279, p(D14)=0.0083*
7C	*KO/KO=6, WT/KO=6*	*Normal distribution*	*t test*	*t(D1-D5)=2.393, t(D1-D14)=5.840*	*p(D1-D5)=0.0378, p(D1-D14)=0.0002*
7D	*KO/KO=6, WT/KO=6*	*Normal distribution*	*t test*	*t=3.1534*	*p=0.0103*
7E	*KO/KO=8, WT/KO=8*	*Normal distribution*	*2-way repeated ANOVA, Bonferroni post hoc*	*F(1,14)=8.077*	*p=0.0131, Pre: p>0.9999, D3: p=0.0039, D5: p=0.0297, D7: p=0.1719, D14: p=0.5095*
7F	*KO/KO=8, WT/KO=8*	*Normal distribution*	*2-way repeated ANOVA, Bonferroni post hoc*	*F(1,14)=10.38*	*p=0.0062, Pre: p>0.9999, D3: p=0.0160, D5: p=0.0118 D7: p=0.6346, D14: p=0.3006*
7G	*KO/KO=6, WT/KO=6*	*Normal distribution*	*Pearson correlation*	*R=-0.1608*	*p=0.6192*
7H	*KO/KO=6, WT/KO=6*	*Normal distribution*	*Pearson correlation*	*R=0.5909*	*p=0.0430*
7I	*KO/KO=6, WT/KO=6*	*Normal distribution*	*Pearson correlation*	*R=-0.6537*	*p=0.0211*

FIGURE 8	**n**	**DATA STRUCTURE**	**TEST USED**	**STATISTIC**	**P VALUE**
8B	*WT=2, KO=3*	*Normal distribution*	*t test*	*t(Il1rl1)=3.242, t(Cd36)=4.785, t(Cnn2)=7.605, t(Colec12)=6.63, t(Ticam)=5.184, t(Fcer1g)=3.261,*	*p(Il1rl1)=0.0478, p(Cd36)=0.0174, p(Cnn2)=0.0047, p(Colec12)=0.007, p(Ticam)=0.0139, p(Fcer1g)=0.0471,*
8C	*WT=6, KO=6*	*Normal distribution*	*t test*	*t=4.607*	*P=0.001*
8D	*WT=6, KO=6, KO+IL-4=6*	*Normal distribution*	*1-way ANOVA, Bonferroni post hoc*	*F=4.516*	*p=0.0292, WT vs KO: p=0.0332, WT vs KO+IL-4: p=0.1477, KO vs KO+IL-4: p>0.9999*
8E	*WT=6, KO=6, KO+IL-4=6*	*Normal distribution*	*2-way repeated ANOVA, Bonferroni post hoc*	*F(2,15)=6.604*	*p=0.0088, WT vs KO: p=0.0120,*

Foot fault					*WT vs KO+IL-4: p=0.0387, KO vs KO+IL-4: p>0.999; Pre: WT vs KO p>0.9999, WT vs KO+IL-4 p>0.9999, KO vs KO+IL-4 p>0.9999; D1: WT vs KO p=0.0016, WT vs KO+IL-4 p=0.0343, KO vs KO+IL-4 p=0.8894; D3: WT vs KO p=0.1645, WT vs KO+IL-4 p>0.9999, KO vs KO+IL-4 p=0.9655; D5: WT vs KO p=0.1997, WT vs KO+IL-4 p=0.0307, KO vs KO+IL-4 p>0.9999;*
8E cylinder	*WT=6, KO=6, KO+IL-4=6*	*Normal distribution*	*2-way repeated ANOVA, Bonferroni post hoc*	*F(2,15)=6.497*	*p=0.0093, WT vs KO: p=0.0129, WT vs KO+IL-4: p=0.0396, KO vs KO+IL-4: p>0.999; Pre: WT vs KO p>0.9999, WT vs KO+IL-4 p>0.9999, KO vs KO+IL-4 p>0.9999; D1: WT vs KO p=0.0073, WT vs KO+IL-4 p=0.0231, KO vs KO+IL-4 p>0.999; D3: WT vs KO p=0.1846, WT vs KO+IL-4 p=0.4820, KO vs KO+IL-4 p>0.9999; D5: WT vs KO p=0.1235, WT vs KO+IL-4 p=0.2626, KO vs KO+IL-4 p>0.9999;*
8F	*WT=6, KO=6, KO+IL-4=6*	*Non normal distribution*	*Spearman correlation*	*R=0.6060*	*p=0.0077*

FIGURE S1	**n**	**DATA STRUCTURE**	**TEST USED**	**STATISTIC**	**P VALUE**
SF1B	*Vehicle=10, IL-4=10*	*Normal distribution*	*2-way repeated ANOVA, Bonferroni post hoc*	*F(1,18)=4.315*	*p(D1)>0.9999, p(D5)=0.0026, p(D14)>0.9999*
SF1C	*Vehicle=10, IL-4=10*	*Normal distribution*	*2-way repeated ANOVA, Bonferroni post hoc*	*F(1,18)=3.708*	*p(D1)=0.5848, p(D5)=0.2032, p(D14)=0.0249*

FIGURE S2	**n**	**DATA STRUCTURE**	**TEST USED**	**STATISTIC**	**P VALUE**
SF2A	*Vehicle=8, IL-4=6*	*Normal distribution*	*2-way repeated ANOVA, Bonferroni post hoc*	*F(1,12)=9.100*	*p=0.0107, Pre: p>0.9999, D3: p=0.0138, D5: p-0.0038, D7: 0.0808, D14: p=0.2089*
SF2B	*Vehicle=8, IL-4=6*	*Normal distribution*	*2-way repeated ANOVA, Bonferroni post hoc*	*F(1,12)=10.34*	*p=0.0074, Pre: p>0.9999, D3: p=0.0184, D5: p=0.0697, D7: p=0.3546, D14: p=0.9295*
SF2C	*Vehicle=8, IL-4=6*	*Normal distribution*	*2-way repeated ANOVA, Bonferroni post hoc*	*F(1,12)=17.16*	*p=0.0014, Pre: p>0.9999, D3: p=0.3189, D5: p=0.0661, D7: 0.0167, D14: 0.0967*
SF2D	*Vehicle=9, IL-4=8*	*Normal distribution*	*2-way repeated ANOVA, Bonferroni post hoc*	*F(1,15)=12.92*	*p=0.0027, Pre: p>0.9999, D3: p=0.0595, D5: p=0.0057, D7: p>0.9999, D14: p>0.9999*
SF2E	*Vehicle=9, IL-4=8*	*Normal distribution*	*2-way repeated ANOVA, Bonferroni post hoc*	*F(1,15)=5.405*	*p=0.0345, Pre: p>0.9999, D3: p=0.0190, D5: p=0.0586, D7: p>0.9999, D14: p>0.9999*

SF2F	*Vehicle=9, IL-4=8*	*Normal distribution*	*2-way repeated ANOVA, Bonferroni post hoc*	*F(1,15)=3.816*	*p=0.0697, Pre: p>0.9999, D3: p>0.9999, D5: p=0.7980, D7: p>0.9999, D14: p>0.9999*

FIGURE S3	**n**	**DATA STRUCTURE**	**TEST USED**	**STATISTIC**	**P VALUE**
SF3B	*Sham=5, d1=5, d3=4, d5=4, d7=3, d14=4*	*Sham, d3 = non normal distribution. D1, d5, d7, d14 =normal distribution*	*1-way ANOVA, Bonferroni post hoc*	*F(4,15)=32*	*p<0.0001 p(D1 vs D3)=0.0177, p(D1 vs D5)<0.0001, p(D1 vs D7)=0.0112, p(D1 vs D14)=0.4244*
SF3C	*Oligodendrocyte, neuron, astrocyte, microglia/macrophage = 5, Isotype = 3*	*Normal distribution*	*t test*	*t(micro/macro)=50.57, t(neuron)=0.05322, t(astrocyte)=2.349, t(oligo)=1.052*	*p(micro/macro)<0.0001, p(neuron)=0.9593, p(astrocyte)=0.0572, p(oligo)=0.3331*
SF3E	*Vehicle: d1=5, d3=4, d5=4; IL-4: d1=4, d3=4, d5=4*	*D3 vehicle = non normal distribution, d1 and d5 vehicle = normal distribution, IL-4 =normal distribution,*	*D1, d5: t test, D3: Mann-Whitney test*	*t(d1)=3.005, U=0, t(d5)=0.1851*	*p(D1)=0,0198, p(D3)=0.0286, p(D5)=0.8592*
SF3G	*Sham=3, D1=3, d3=4, d5=5, d7=5, d14=6*	*Normal distribution*	*t test*	*t(D3 vs D1)=8.602, t(D5 vs D1)=10.73, t(D7 vs D1)=3.854, t(D14 vs D1)=3.472*	*p(D3 vs D1)=0.0004, p(D5 vs D1) < 0.0001, p(D7 vs D1)=0.0084, p(D14 vs D1)=0.0104*

FIGURE S4	**n**	**DATA STRUCTURE**	**TEST USED**	**STATISTIC**	**P VALUE**
SF4B	*WT=8, KO=8, KO+IL-4 =6*	*Normal distribution*	*2-way repeated ANOVA, Bonferroni post hoc*	*F(2,19)=1.906*	*p=0.1761*
SF4C	*WT=6, KO=6, KO+IL-4=6*	*Normal distribution*	*Pearson correlation*	*R=0.7825*	*p=0.0001*
SF4D	*WT=6, KO=6, KO+IL-4=6*	*Normal distribution*	*Pearson correlation*	*R=0.3283*	*p=0.1836*
SF4E	*WT female =9, KO female =12*	*Normal distribution*	*2-way repeated ANOVA, Bonferroni post hoc*	*F(1,19)=4.494;*	*p=0.0474, Pre p>0.9999, D3 p=0.1299, D5 p=0.8136, D7 p=0.7206, D14 p>0.9999;*
SF4E	*WT female =9, KO female =12*	*Normal distribution*	*2-way repeated ANOVA, Bonferroni post hoc*	*F(1,19)=9.76*	*p=0.0056, Pre p>0.9999, D3 p=0.4236, D5 p=0.2335, D7 p=0.2101, D14 p=0.0856*

FIGURE S5	n	DATA STRUCTURE	TEST USED	STATISTIC	P VALUE
SF6B	*KO: 0.5h=6, 1h=7, 2h=10, 4h=8, WT: 0.5h=6, 1h=8, 2h=10, 4h=8,*	*Normal distribution*	*t test*	*t(0.5h)=4.648, t(1h)=6.862, t(2h)=5.990, t(4h)=5.623,*	*p(0.5h)=0.0009, p(1h)<0.0001, p(2h)<0.0001, p(4h)<0.0001,*

References

1. Townsend MJ, Fallon PG, Matthews DJ, Jolin HE, & McKenzie AN (2000) T1/ST2-deficient mice demonstrate the importance of T1/ST2 in developing primary T helper cell type 2 responses. *The Journal of experimental medicine* 191(6):1069-1076.
2. National Research Council (2011) *Guide for the Care and Use of Laboratory Animals* (National Academies Press, Washington, DC) 8th Ed.
3. Chang CF, Massey J, Osherov A, Angenendt da Costa LH, & Sansing LH (2020) Bexarotene Enhances Macrophage Erythrophagocytosis and Hematoma Clearance in Experimental Intracerebral Hemorrhage. *Stroke* 51(2):612-618.
4. Zhao X*, et al.* (2015) Cleaning up after ICH: the role of Nrf2 in modulating microglia function and hematoma clearance. *Journal of neurochemistry* 133(1):144-152.
5. Dang G*, et al.* (2017) Early Erythrolysis in the Hematoma After Experimental Intracerebral Hemorrhage. *Translational stroke research* 8(2):174-182.
6. Xia Y*, et al.* (2018) Tissue plasminogen activator promotes white matter integrity and functional recovery in a murine model of traumatic brain injury. *Proceedings of the National Academy of Sciences of the United States of America* 115(39):E9230-E9238.
7. Zhang J*, et al.* (2019) Preconditioning with partial caloric restriction confers long-term protection against grey and white matter injury after transient focal ischemia. *J Cereb Blood Flow Metab* 39(7):1394-1409.
8. Shi Y*, et al.* (2017) Endothelium-targeted overexpression of heat shock protein 27 ameliorates blood-brain barrier disruption after ischemic brain injury. *Proc Natl Acad Sci U S A* 114(7):E1243-E1252.
9. Gan Y*, et al.* (2012) Transgenic overexpression of peroxiredoxin-2 attenuates ischemic neuronal injury via suppression of a redox-sensitive pro-death signaling pathway. *Antioxid Redox Signal* 17(5):719-732.
10. Hu X*, et al.* (2008) Macrophage antigen complex-1 mediates reactive microgliosis and progressive dopaminergic neurodegeneration in the MPTP model of Parkinson's disease. *J Immunol* 181(10):7194-7204.
11. Schallner N*, et al.* (2015) Microglia regulate blood clearance in subarachnoid hemorrhage by heme oxygenase-1. *The Journal of clinical investigation* 125(7):2609-2625.
12. Yang Y*, et al.* (2017) ST2/IL-33-Dependent Microglial Response Limits Acute Ischemic Brain Injury. *J Neurosci* 37(18):4692-4704.